Int j simul model 22 (2023) 4, 701-711
Original scientific paper

HIGH-SPEED BEARING DYNAMICS AND APPLICATIONS IN PRODUCTION LINES

Zhang, L. J.; Yang, S. J.[#]; Wang, S. J.; Zeng, Y. M.; Hua, W. C. & Li, G. L.
School of Mechanical and Electronic Engineering, Northwest A & F University; Yangling 712100, China
E-Mail: yangshanju@nwafu.edu.cn ([#] Corresponding author)

Abstract
This study presents a novel approach to simulating and monitoring the dynamic performance of high-speed bearings, a critical component in automated industrial production for system efficiency and safety. The newly developed theoretical framework allows for detailed analysis of dynamic responses in these bearings, especially under high-speed conditions. The Short-Time Fourier Transform (STFT) is used to capture time-frequency domain characteristics, while real-time condition monitoring is achieved through a deep learning-based Convolutional Neural Network, enhanced by a multi-head attention mechanism. This method enables managing large datasets, real-time surveillance, and accurate prediction of bearing conditions. Ultimately, this approach provides an innovative perspective for fault diagnosis and performance assessment of high-speed bearings in complex production environments.
(Received in June 2023, accepted in September 2023. This paper was with the authors 6 weeks for 2 revisions.)

Key Words: High-Speed Bearings, Dynamic Performance Simulation, Equilibrium Equations, Time-Frequency Domain Feature Extraction, Deep Learning, Real-Time Condition Monitoring

1. INTRODUCTION

In the realm of industrial development over recent decades, the evolution of automation and precision machinery manufacturing has been paralleled by the ascent of high-speed bearings as quintessential components within contemporary production frameworks [1-4]. These bearings have been broadly implemented in an array of sophisticated equipment, including but not limited to aero-engines, high-speed railway systems, and CNC machine tools, establishing themselves as foundational to the seamless operation of such apparatuses [5, 6]. It has been discerned that the operational characteristics of high-speed bearings are inextricably linked with the efficiency, stability, and durability of the machinery systems at large, thereby positioning the analysis of their dynamic performance as a topic of considerable engineering relevance and theoretical significance [7-9]. In response to the industry's stringent criteria for the dependability and serviceability of high-speed bearings, the pursuit of dynamic simulation analyses has been recognized as a field of critical research necessity.

Simulation of dynamic performance has been acknowledged as a prescient technique for the prediction and diagnosis of potential issues in high-speed bearings, enabling the identification of faults prior to their manifestation and guiding maintenance personnel towards precise interventions [10, 11]. This proactive approach not only extends the service life of the bearings but also minimizes unplanned downtime in production lines, concurrently reducing maintenance costs and enhancing production efficiency [12-15]. Consequently, the simulation and analysis of the dynamic characteristics of high-speed bearings are not only imperative in the design and manufacturing phases but also constitute a vital component within modern production line maintenance and management systems [16, 17].

Existing studies, however, have been predominantly concentrated on macroscopic mechanical models and empirical formulas, with scant research delving into the intricate dynamics within bearings at a microscopic level [18, 19]. Conventional methodologies exhibit clear deficiencies in addressing the nonlinear and non-stationary signals generated by high-

speed rotations, leading to simulations that diverge significantly from actual conditions [20, 21]. Moreover, the real-time aspect represents a substantial challenge, with previous research falling short of the requirements for real-time monitoring and rapid feedback of high-speed bearing dynamics.

In response to these challenges, the mechanical characteristics and internal dynamic responses of bearings under high-velocity rotations have been simulated. Moreover, the employment of STFT, an advanced signal processing technique, has facilitated the effective extraction of time-frequency domain features under complex working conditions. These features are posited to precisely reflect and predict the operational state of the bearings. Finally, the introduction of an innovative, deep learning-based, real-time monitoring technique, which integrates multi-scale CNN with a multi-head attention mechanism, has significantly enhanced the efficiency and accuracy of the model in processing voluminous high-speed bearing data. The innovations and breakthroughs presented herein markedly advance the field of high-speed bearing dynamic performance simulation and offer robust technological support for their application in modern production lines, heralding profound industrial and research implications.

2. TIME-FREQUENCY DOMAIN DYNAMIC FEATURE EXTRACTION OF HIGH-SPEED BEARINGS

An in-depth investigation into the extraction of dynamic features in the time-frequency domain for high-speed bearings constitutes the initial phase of this research. Time-frequency analysis methods, such as the STFT, are employed to capture subtle changes and complex nonlinear behaviours in the rapidly changing operational environment of the bearings. Such feature extraction is capable of revealing details that may be overlooked in standard frequency domain analysis, including instantaneous frequency variations, regions of energy concentration, and their temporal evolution. These details are crucial for understanding and predicting the performance of high-speed bearings in actual working conditions.

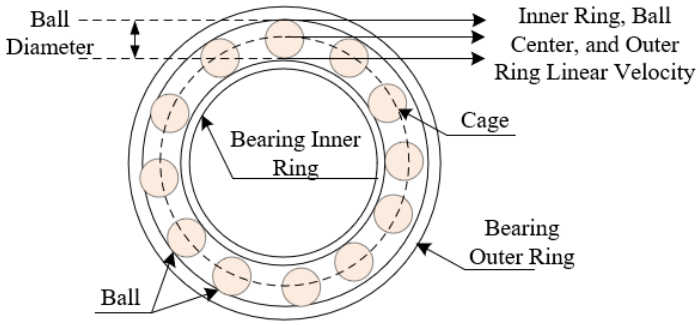

Figure 1: Structure of a bearing.

Fig. 1 presents a schematic diagram of a bearing structure. The signals produced by high-speed bearings during operation are typically non-stationary, with frequency characteristics that vary over time. The STFT applies a sliding window of short temporal width to the time-domain signal, enabling local Fourier Transform of the signal. This process not only yields the frequency components but also identifies the precise times at which these frequencies occur. Capturing and analysing transient features, impact responses, or fault signals in high-speed rotating bearings is of paramount importance. This research opts for the STFT to extract the dynamic features in the time-frequency domain of high-speed bearings, with a detailed description of the extraction process provided below.

The STFT is utilized to analyse the frequency and phase content of signals that vary over time. This method involves segmenting a long-duration signal into shorter time segments, each multiplied by a sliding window function. Each segment can be considered as a quasi-stationary

state of the signal within that time frame, and Fourier Transform applied to each segment yields the corresponding spectrum. Thus, the STFT generates a spectrum for each short time segment, allowing observation of how the signal's frequency changes over time. Assuming the complex conjugate is represented by *, the following equation defines the STFT of the signal $x(y)$:

$$BHDY_X(t,d) = \int_{-\infty}^{\infty} \left[x(y')\varepsilon^*(y'-y)\right] e^{-k2\pi dy'} fy' \tag{1}$$

The STFT encompasses both forward and inverse transformations. In time-frequency domain analysis, to fully reconstruct the original signal from the STFT, the window function and the overlap of the sliding windows must possess certain characteristics, such as meeting the Kolmogorov reconstruction condition. Hence, through the inverse STFT, the original dynamic signal can theoretically be reconstructed without loss. The reconstruction formula for signal $x(y)$ is given as follows:

$$o(i) = \int_{-\infty}^{\infty}\int_{-\infty}^{\infty} BHDY_X(y,d)h(i-y)r^{k2\pi di} fyfd \tag{2}$$

Upon integrating over frequency d, the result is:

$$o(i) = x(i)\int_{-\infty}^{\infty} \varepsilon^*(i-y)h(i-y)fy = x(i)\int_{-\infty}^{\infty} \varepsilon^*(y)h(y)fy \tag{3}$$

The complete reconstruction of the dynamic motion signal of high-speed bearings is a process in which the original state of the signal can be accurately restored after time-frequency analysis. To achieve a complete reconstruction of the dynamic motion signal of high-speed bearings, the sampling frequency of the signal must satisfy the Nyquist theorem, and an appropriate window function must be selected with a rational design for the window overlap strategy, ensuring that $o(i) = x(i)$. Assuming the analysis window is represented by $\varepsilon(y)$, the composite window by $h(y)$, and the dual window of the analysis window by $\varepsilon^*(y)$, then there is:

$$\int_{-\infty}^{\infty} \varepsilon^*(y)h(y)fy = 1 \tag{4}$$

Given that the signals processed by computers are discrete, the continuous STFT must be converted into a Discrete-Time Short-Time Fourier Transform (DTSTFT). This necessitates appropriate sampling of the signal and the selection of a sampling frequency to ensure the frequency content of the signal is adequately represented. Typically, this sampling frequency should be at least twice the highest frequency component in the signal, to avoid aliasing as per the Nyquist Sampling Theorem. Assuming the window function is denoted by $q[l]$, the following defines the DTSTFT for the dynamic signal of high-speed bearings:

$$BHDY(b,\mu) = \sum_{l=-\infty}^{\infty} x[b+l]q[l]e^{-k\mu dl} \tag{5}$$

Supposing the length of the window is denoted by M, for the DTSTFT, the values of l should satisfy $q[l] \neq 0 (0 \leq l \leq M\text{-}1)$. Outside the interval $[0, M\text{-}1]$, $q[l] = 0$. Hence, the previous formula can be modified to:

$$BHDY(b,\mu) = \sum_{l=0}^{M-1} x[b+l]q[l]e^{-k\mu dl} \tag{6}$$

In the DTSTFT, for each time window, the Fourier Transform's output is a set of complex numbers that represent the signal's frequency components and their phase information within that time window. These complex numbers are sampled equidistantly in the frequency domain, with the interval determined by the sampling frequency. The results are commonly represented as a time-frequency plot, which can be used to visually observe the frequency distribution of the signal over time. Assuming $BHDY(b,\mu)$ undergoes B equidistant frequency samplings, with the sampling interval denoted by $\mu_d = 2\tau d / B$, then it follows that:

$$BHDY(b,d) = BHDY(b, 2\tau d/B) = \sum_{l=0}^{M-1} x[b+l]q[l]e^{-k(b,2\tau d/B)dl}, 0 \le d \le B-1 \quad (7)$$

$BHDY(b,d)$ is the Discrete Fourier Transform of the windowed sequence $x[b+l]\,q[l]$. Once the time-frequency plot is obtained, performing the Inverse Discrete Fourier Transform (IDFT) on the data for each time window enables the frequency components to be recombined, reconstructing the time domain signal segments corresponding to each time window.

3. REAL-TIME MONITORING OF HIGH-SPEED BEARINGS BASED ON DEEP LEARNING

Real-time monitoring plays an essential role in enhancing the stability of production lines and reducing unplanned downtime. Deep learning models are capable of autonomously learning profound representations of bearing conditions from complex time-frequency domain features. These representations are more abstract and refined than those of traditional monitoring methods, providing a more accurate reflection of the health status and potential failure modes of bearings. In this study, the nonlinear relationships between the motion signals of high-speed bearings at different operating times and their dynamic performance are deciphered through the powerful data processing capabilities of multi-scale CNN. Fig. 2 illustrates the flow for real-time monitoring of high-speed bearings based on deep learning.

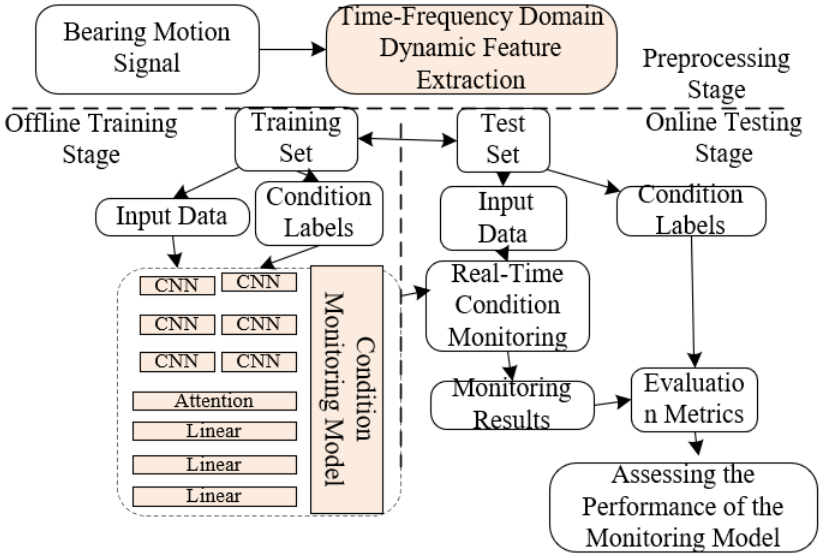

Figure 2: Flow of real-time monitoring of high-speed bearings based on deep learning.

To fully harness the complex signals produced during the operation of high-speed bearings, the constructed deep learning-based model for real-time condition monitoring of high-speed bearings incorporates input data with four dimensions. These dimensions include the time dimension, depth/channel, and two spatial scale dimensions. Data of the time dimension are derived from continuous sensor signals monitoring the high-speed bearings, recorded over a defined time window. This dimension represents the duration of data collection, capturing the dynamic behaviours and trend variations of the bearing over time. It is crucial for understanding how bearing performance evolves, particularly for capturing periodic or transient anomalies. The depth/channel dimension data are sourced from multiple sensors or multiple features extracted from the original signals, such as vibration, acoustic emission sensors, and temperature sensors. This dimension can be perceived as the depth of features representing multiple extracted attributes from bearing signals, like different frequency components of vibration data, temperature, load, and other sensor data. Within the CNN context, this can also

be understood as the number of feature maps extracted by various filters, denoted as the channel count. Data pertaining to the spatial scale originate from STFT, which convert time-series signals into a spatially scaled feature representation. In the context of this study, this typically refers to the two-dimensional representation of features extracted from time-frequency domain analysis. These two dimensions represent time slices within a time window and the corresponding frequency components, thus forming a time-frequency spectrum.

For the fine control requirements of the deep learning model training process in monitoring the dynamic performance of high-speed bearings, the adaptive gradient algorithm along with the RMSProp algorithm have been employed to adjust the learning rate of parameters. Let the learning rate be denoted by λ and the gradient by ∇M. The formula for updating parameters via gradient descent utilized by the model is given below:

$$q = q - \lambda \nabla M \tag{8}$$

The Adagrad algorithm, by assigning an independent learning rate to each parameter, enhances the model's performance on sparse data effectively. This proves particularly vital when handling the nonlinear and non-stationary features in high-speed bearing motion signals, which contain sparse but significant information on anomalies or failures. The adjustment is made as follows:

$$e_y = e_{y-1} + \nabla M \otimes \nabla M \tag{9}$$

$$q_y = q_{y-1} - \frac{\lambda}{\gamma + \sqrt{e_y}} \otimes \nabla M \tag{10}$$

From the derivation above, it is understood that there is a problem where the Adagrad learning rate decreases monotonically over time, potentially leading to premature cessation of training. The RMSProp algorithm serves as an improvement to Adagrad by introducing a moving average of the squared gradient to adjust the learning rate, effectively addressing the aforementioned issue. The adjustment by RMSProp is as:

$$e_y = \vartheta c_{y-1} - (1-\vartheta)\nabla M \Phi \nabla M \tag{11}$$

To ensure that the model performs effectively and with high accuracy in monitoring the subtle dynamic characteristics of high-speed bearings, the decay method of the RMSProp algorithm is combined with the concept of momentum. The adjustment is therefore made as follows:

$$e_y = \vartheta c_{y-1} - (1-\vartheta)\nabla M \tag{12}$$

$$e_y = \vartheta' c_{y-1} - (1-\vartheta')\nabla M \Phi \nabla M \tag{13}$$

Furthermore, bias correction is applied to variables c_y and e_y to eliminate the effects of bias:

$$\hat{c}_y = \frac{c_y}{1-(\vartheta)^y} \tag{14}$$

$$\hat{e}_y = \frac{c_y}{1-(\vartheta')^y} \tag{15}$$

In practical applications involving high-speed bearings, bearings are subjected to various loads, speeds, and temperature conditions. These conditions influence the vibration signal patterns of the bearings. Complex changes in operational conditions bring about diverse failure characteristics and noise, hence the need for a monitoring model with robust feature extraction and adaptability capabilities. To address the aforementioned challenges, a multi-head attention mechanism is incorporated into the constructed multi-scale CNN model. Fig. 3 presents the calculation flow of the multi-head attention mechanism.

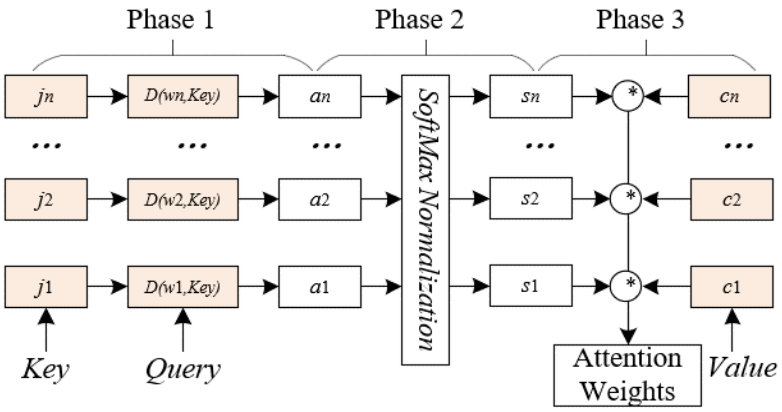

Figure 3: Calculation flow of the multi-head attention mechanism.

In the practical operational conditions of high-speed bearings, the multi-head attention mechanism allows the model to effectively distinguish and utilize complex signal characteristics that arise under different operating conditions, especially in vibration patterns under variations in speed, load, or temperature. This mechanism significantly enhances the model's expressive capacity and diagnostic accuracy, particularly when dealing with bearing signals that exhibit rich time-varying features, which is crucial for the early detection of potential faults and anomalies. Fig. 4 presents the dynamic simulation analysis process for high-speed bearings.

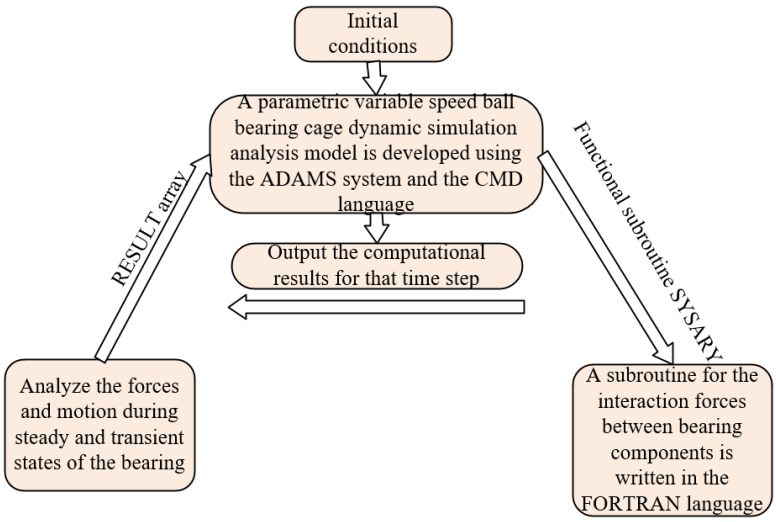

Figure 4: Dynamic simulation analysis process for high-speed bearings.

4. SIMULATION EXPERIMENT RESULTS AND ANALYSIS

Fig. 5 presents the maximum slip rates of high-speed bearing balls under both uniform and variable velocity conditions. The slip rate is defined as the ratio of the sliding velocity of the ball relative to the raceway to its theoretical rolling velocity, an important metric influencing the wear rate and service life of the bearing. In Fig. 5 a, fluctuations in the slip rate over time are observed to be frequent but of small magnitude. Such fluctuations may be attributed to irregular contact between the balls and the raceway, arising from minor manufacturing imperfections or assembly errors within the bearing. The presence of these fluctuations indicates that even under uniform velocity conditions, the operation of the bearing is not entirely uniform, yet the overall magnitude of change remains limited, reflecting relatively stable dynamic performance. In Fig. 5 b, a significant increase in slip rate is observed under variable

velocity conditions, particularly at the peak in the middle of the graph, indicating a considerable elevation in slip rate during speed transitions. Sharp peaks such as these may result from increased relative velocity differences between the balls and the raceway during acceleration or deceleration phases. Elevated slip rates may lead to accelerated wear of the bearing, thus monitoring and controlling slip rates in such states is crucial for ensuring bearing lifespan and performance. From these two graphs, it is evident that the model constructed in this study is capable of capturing the dynamic changes in slip rates of high-speed bearings under both uniform and variable speed conditions, proving the model's effectiveness. Notably, under variable velocity conditions, the model accurately identifies high slip rate events, which is highly beneficial in practical applications as it can aid engineers or maintenance personnel in identifying operational conditions that may lead to excessive wear or failure, allowing for the implementation of appropriate measures.

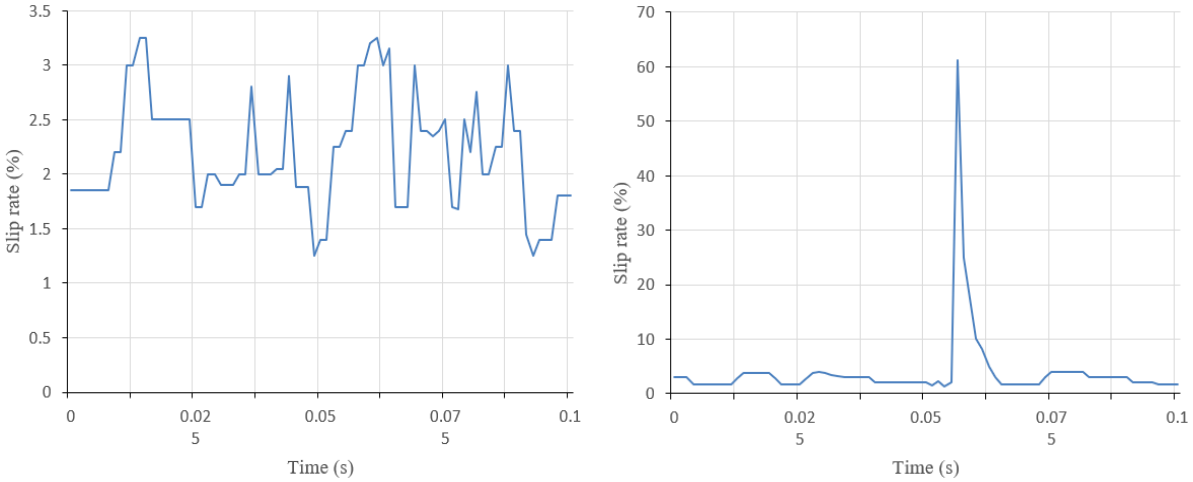

a) Uniform velocity condition b) Variable velocity condition

Figure 5: Simulation curves of maximum slip rates of high-speed bearing balls.

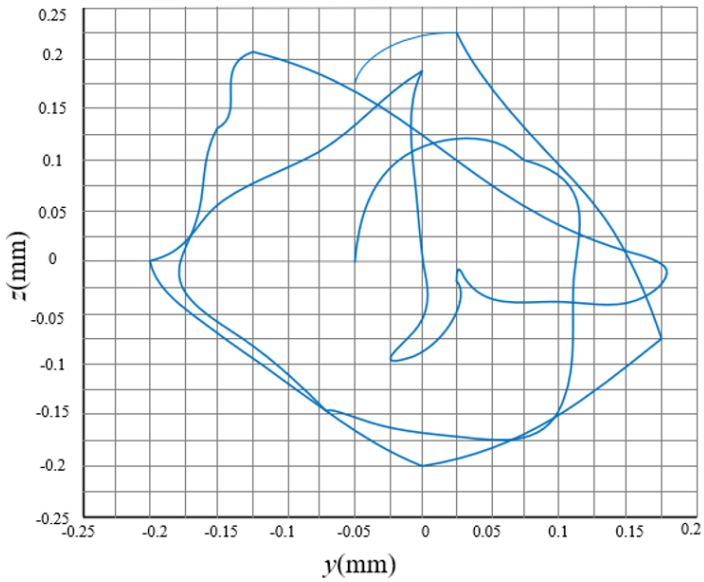

Figure 6: Simulated trajectory of the mass centre of a high-speed bearing.

Fig. 6 depicts the simulated trajectory of the mass centre of a high-speed bearing. It is observed from the figure that the mass centre trajectory is not a single, regular shape but presents a complex and irregular path. This could imply the presence of dynamic imbalance or other forms of irregular motion during the bearing's operation. The demonstrated trajectory,

being varied and complex, may indicate the intricate interactions among the internal components of the bearing, such as changes in contact forces between the balls and the inner and outer races, or variations in lubrication conditions. The sensitivity of the mass centre trajectory is crucial for detecting the health status of the bearing. Any deviations from the normal trajectory could be indicative of potential issues, such as bearing damage or end of service life. The irregularity and complexity of the bearing's mass centre trajectory, as shown in the figure, suggest that the model constructed in this research is capable of capturing the subtle dynamic changes during the bearing's operation. The model effectively reflects the variations in the internal mechanical characteristics of the bearing, as well as possible changes in its health status. This capability is essential for predicting and diagnosing bearing failures, planning maintenance, and avoiding unplanned downtime and the associated cost expenditures.

Fig. 7 presents the real-time status monitoring results for high-speed bearings under constant and variable speed conditions, illustrated by the estimation of Remaining Useful Life (*RUL*). The abscissa represents time in minutes, while the ordinate represents the normalized *RUL* values, with 1 indicating a new or fully functional state, and 0 indicating the threshold for failure. The real-time monitoring results displayed in Fig. 7 a, when compared with the baseline, indicate that the model is capable of closely following the actual equipment life curve, suggesting accurate predictive capabilities. Despite some fluctuations observed in Fig. 7 b, the *RUL* predicted by the model maintains a good consistency with the baseline. These fluctuations are likely due to the uncertainties and complexities introduced by variable speed operations in actual working conditions. Therefore, the model constructed in this study is effective in monitoring the real-time status of high-speed bearings and reliably predicting their *RUL* under both constant and variable speed conditions. Particularly under constant speed conditions, the model's prediction aligns almost perfectly with the actual life, and even with fluctuations under variable speed conditions, the model still captures the trend and makes reasonable predictions.

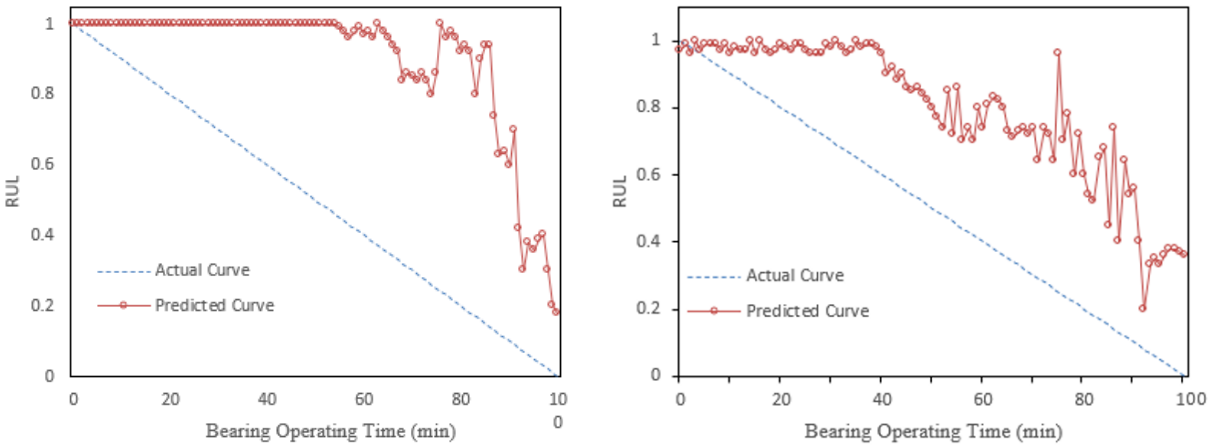

a) Uniform velocity condition b) Variable velocity condition

Figure 7: Real-time status monitoring results for high-speed bearings.

The study further incorporates real-time status monitoring techniques based on deep learning, employing a multi-scale CNN combined with a multi-head attention mechanism. This model is designed to efficiently process a vast array of data, thereby enabling the real-time monitoring and accurate prediction of bearing status. Fig. 8 illustrates the instantaneous frequency prediction results for high-speed bearings under varying operational time conditions. The figure presents two curves; the measured values (depicted by the blue dashed line) and the predicted values (depicted by the red solid line). It is observed from the figure that the predicted curve closely follows the general trend of the actual measured curve, indicating that the model is capable of capturing the trend of bearing instantaneous frequency changes over time effectively. For the majority of the operational duration, the predicted values remain in close

proximity to the measured values, with only slight deviations at certain points. These deviations could be attributed to the model's precision, noise within the data, or the non-linear characteristics present under bearing operational conditions. There has been no significant decrease in prediction accuracy over time, suggesting that the model is stable and reliable. The close correspondence between actual and predicted values, as depicted in the figure, demonstrates the robust modelling capability of the constructed model and its high predictive accuracy for the behaviour of high-speed bearings. Such performance of the model is crucial for real-time monitoring and fault diagnosis of high-speed bearings, ensuring their normal operation and timely detection and prevention of potential failures.

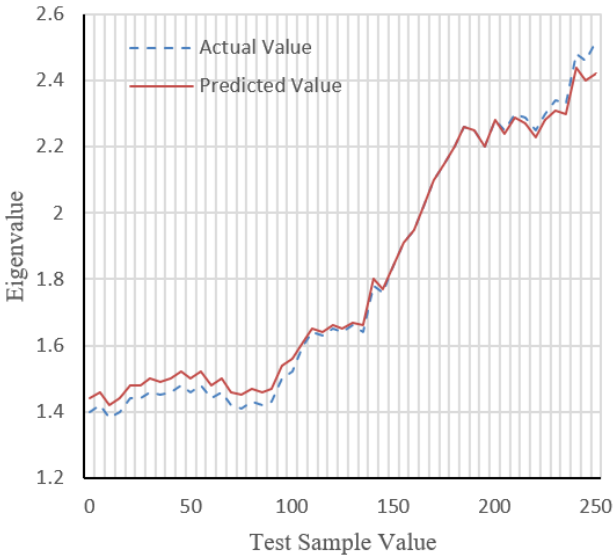

Figure 8: Instantaneous frequency prediction results for high-speed bearings under varying operational time conditions.

Table I: Performance of high-speed bearing real-time condition monitoring models for different models.

Model	***MAE***	***RMSE***	**Time** (s)
Prior to the introduction of the adaptive gradient algorithm	12.895	13.887	71.564
Prior to the introduction of RMSProp algorithm	2.235	7.286	64.586
Prior to the introduction of multi-head attention mechanism	15.962	16.968	55.362
The proposed model	1.296	0.985	53.287

Table I presents a comparative analysis of the performance of various models in the task of real-time condition monitoring of high-speed bearings, including *MAE*, *RMSE*, and model execution time. Significant reductions in both *MAE* and *RMSE* were observed for the proposed model compared to models without the implementation of the adaptive gradient algorithm and the RMSProp algorithm, indicating that improvements in optimization algorithms have a significant positive impact on accuracy. The introduction of the multi-head attention mechanism led to a substantial decrease in the values of *MAE* and *RMSE*, demonstrating the mechanism's significant enhancement of the model's ability to recognize complex data patterns, thereby improving predictive performance. The analysis underscores the marked improvement of the study's model over several other models in terms of error metrics, and a reduction in execution time while maintaining or even enhancing accuracy. The notable decrease in *MAE* and *RMSE* underscores the model's high accuracy and reliability, while the shorter execution time suggests the model's suitability for real-time monitoring scenarios. Thus, the efficacy of the proposed model is emphasized, displaying superior performance in the real-time condition monitoring of high-speed bearings.

5. CONCLUSION

This study has been concentrated on the condition monitoring and performance prediction of high-speed bearings, with a particular focus on their behaviour under constant and variable speed conditions. A deep learning model has been constructed through a series of experiments and analyses, employing a multi-scale CNN and a multi-head attention mechanism to enhance the capability of processing vast amounts of data and achieving accurate predictions. The maximum slip rate of bearing balls, under both constant and variable speed states, has been quantified through experimental methods. Analyses of provided diagrams indicate greater fluctuations in slip rates under variable speeds, underscoring the importance and complexity of bearing condition monitoring under varying operational conditions. Analysis of mass centre trajectory diagrams has revealed the dynamic characteristics of bearings during operation, elucidating the dynamic stability and potential non-linear features of bearings. Simulation results have demonstrated that the deep learning model is capable of real-time condition monitoring of high-speed bearings, with synthetic time-frequency diagrams showing improvements in accuracy over conventional time-frequency representations. A comparison of different models' performances has shown that the model described herein exhibits lower errors and shorter execution times across various metrics, indicative of its superior predictive capabilities and efficiency. Significant improvements in evaluative metrics such as *RMSE* and *MAE*, along with the accuracy and real-time nature demonstrated by the experimental data, emphasize the effectiveness of the constructed model.

The research detailed in this article has experimentally validated the efficacy and reliability of the proposed model. Its performance in terms of accuracy, efficiency, and real-time monitoring capabilities attests to its potential application in the field of high-speed bearing condition monitoring. The employment of a multi-scale CNN has enhanced the ability to analyse time-frequency data, while the multi-head attention mechanism has improved the capture of significant features within the data – both key factors in the model's high-performance realization. Overall, the deep learning model established in this article offers an efficient and accurate solution for the health monitoring and maintenance of high-speed bearings, which is of significant relevance for practical industrial applications.

ACKNOWLEDGEMENTS

This paper was supported by Key R & D project of Shaanxi Province (Grant No.: K4040121274).

REFERENCES

[1] Zhao, X.; Zhang, Y. (2023). Tribological and dynamic performance analysis of rolling bearings with varied surface textures operating under lubricant contamination, *Wear*, Vols. 532-533, Paper 205109, 17 pages, doi:10.1016/j.wear.2023.205109

[2] Ambrozkiewicz, B.; Litak, G.; Georgiadis, A.; Syta, A.; Meier, N.; Gassner, A. (2021). Effect of radial clearance on ball bearing's dynamics using a 2-DOF model, *International Journal of Simulation Modelling*, Vol. 20, No. 3, 513-524, doi:10.2507/IJSIMM20-3-568

[3] Smagala, A.; Kecik, K. (2021). Nonlinear dynamics analysis of a rolling bearing, *Journal Européen des Systèmes Automatisés*, Vol. 54, No. 1, 21-26, doi:10.18280/jesa.540103

[4] Zheng, X. (2023). Temperature field analysis of high-speed bearings considering frictional heat and interactive effects, *International Journal of Heat and Technology*, Vol. 41, No. 2, 407-414, doi:10.18280/ijht.410215

[5] Premrov, M.; Ber, B.; Kozem Šilih, E. (2021). Study of load-bearing timber-wall elements using experimental testing and mathematical modelling, *Advances in Production Engineering and Management*, Vol. 16, No. 1, 67-81, doi:10.14743/apem2021.1.385

[6] Li, H.; Geng, H.; Li, X.; Qi, L. (2022). The limiting static and dynamic performance of foil bearings, *Proceedings of the Institution of Mechanical Engineers, Part J: Journal of Engineering Tribology*, Vol. 236, No. 1, 205-213, doi:10.1177/13506501211053504
[7] Wei, C.; Liao, G.; Wang, W.; Xu, J.; Liu, K. (2023). Transient tribo-dynamic performance of journal bearings considering wear behavior during start-up, *Proceedings of the Institution of Mechanical Engineers, Part J: Journal of Engineering Tribology*, Vol. 237, No. 9, 1809-1825, doi:10.1177/13506501231187316
[8] Urbiola-Soto, L. (2021). Influence of manufacturing variation on the dynamic and tribological performance of tilting pad journal bearings, *Journal of Engineering for Gas Turbines and Power*, Vol. 143, No. 6, Paper 061017, 15 pages, doi:10.1115/1.4049205
[9] Cui, H.; Wang, Y.; Yue, X.; Li, Y.; Jiang, Z. (2019). Numerical analysis of the dynamic performance of aerostatic thrust bearings with different restrictors, *Proceedings of the Institution of Mechanical Engineers, Part J: Journal of Engineering Tribology*, Vol. 233, No. 3, 406-423, doi:10.1177/1350650118780599
[10] Chen, W.; Hao, Y. F. (2022). A combined service optimization and production control simulation system, *International Journal of Simulation Modelling*, Vol. 21, No. 4, 684-695, doi:10.2507/IJSIMM21-4-CO17
[11] Zhao, C.; Zhang, Q.; Wang, C.; Peng, H. (2023). Digital twin based bearing fault simulation modeling strategy and display dynamics, *2023 6th International Symposium on Autonomous Systems* (*ISAS*), 5 pages, doi:10.1109/ISAS59543.2023.10164348
[12] Li, X.; Zhang, Z.-J. (2023). Research on characteristics of tilting pad bearing based on FLUENT-UDF simulation method, *Third International Conference on Mechanical Design and Simulation (MDS 2023)*, Proc. Vol. 12639, Paper 1263934, 745-753, doi:10.1117/12.2682081
[13] Chi, F.-L.; Yang, X.-Y. (2022). Research on simulation of motor bearing fault diagnosis based on auto-encoder, *Sixth International Conference on Electromechanical Control Technology and Transportation (ICECTT 2021)*, Proc. Vol. 12081, Paper 1208105, 20-28, doi:10.1117/12.2623848
[14] Wajnert, D.; Tomczuk, B. (2022). Two models for time-domain simulation of hybrid magnetic bearing's characteristics, *Sensors*, Vol. 22, No. 4, Paper 1567, 15 pages, doi:10.3390/s22041567
[15] Muchammad, M.; Wibowo, D. D. P.; Tauviqirrahman, M.; Setiyana, B.; Yohana, E.; Jamari, J. (2022). Investigation of the influence of turbulence to tribological performance on smooth and multistep journal bearing with hydrodynamics simulation, *Frontiers in Mechanical Engineering*, Vol. 8, Paper 946074, 12 pages, doi:10.3389/fmech.2022.946074
[16] Han, J.-C.; Li, Y.; Xiong, F. (2022). Modeling and simulation of hybrid magnetic bearing as physical model in Simscape, *2022 IEEE 5th International Conference on Electronics Technology (ICET)*, 386-389, doi:10.1109/ICET55676.2022.9824056
[17] Pan, C.; Wang, C.; Zhao, Y.; Cao, G. (2022). Study on design and simulation of a novel isolator cylindrical roller bearing, *Journal of Mechanical Science and Technology*, Vol. 36, No. 8, 3851-3862, doi:10.1007/s12206-022-0708-3
[18] Liu, J.; Xu, Z. (2022). A simulation investigation of lubricating characteristics for a cylindrical roller bearing of a high-power gearbox, *Tribology International*, Vol. 167, Paper 107373, 13 pages, doi:10.1016/j.triboint.2021.107373
[19] Miao, J.-G.; Li, M.-Y.; Deng, C.-Y.; He, M.-G.; Miao, Q. (2023). Rolling bearing fault diagnosis for a non-ideal dataset based on finite element simulation and transfer learning, *Chinese Journal of Scientific Instrument*, Vol. 44, No. 4, 28-39
[20] Kuncoro, C. B. D.; Oscar, R.; Liu, C.-C.; Chen, C.-Y.; Hung, K.-S.; Kuan, Y.-D. (2021). Modeling, analysis, and simulation of auxiliary bearing for high-speed rotating machinery, *Sensors and Materials*, Vol. 33, No. 10, 3581-3601, doi:10.18494/SAM.2021.3582
[21] Proksch, D.; Stütz, L.; Krotsch, J.; Höfig, B.; Kley, M. (2021). Development of a digital twin for an induction motor bearing voltage simulation, *2021 IEEE Jordan International Joint Conference on Electrical Engineering and Information Technology (JEEIT)*, 103-107, doi:10.1109/JEEIT53412.2021.9634143